

**THERMAL INERTIA AND CONDUCTIVITY MEASUREMENTS OF MARS ANALOG SAMPLES.** A. A. Ahern<sup>1</sup>, A. D. Rogers<sup>1</sup>, R. J. Macke<sup>2</sup>, B. J. Thomson<sup>3</sup>, R. Kronyak<sup>4</sup>, G. Peters<sup>4</sup>, E. Carey<sup>4</sup>. <sup>1</sup>Stony Brook University Department of Geosciences, Earth and Space Science Building, Stony Brook, NY 11767 (*alexandra.ahern@stonybrook.edu*). <sup>2</sup>Vatican Observatory, V-00120, Vatican City State. <sup>3</sup>Department of Earth and Planetary Sciences, University of Tennessee Knoxville, Knoxville, TN 37996. <sup>4</sup>NASA Jet Propulsion Laboratory, Pasadena, CA 91109.

**Introduction:** Thermal inertia ( $I$ ) is the intrinsic property of a material that describes how efficiently that material can store, conduct, and re-radiate heat. It is given by:

$$I = \sqrt{k\rho c} \quad (1)$$

where  $k$  is the bulk thermal conductivity (W/mK),  $\rho$  is the bulk density (g/cm<sup>3</sup>), and  $c$  is the specific heat (J/K);  $I$  has units of J/m<sup>2</sup>Ks<sup>1/2</sup>. At Mars atmospheric pressures (1-10 mbar), thermal inertia is dominated by the effects of thermal conductivity, which in turn is determined by the physical characteristics of near subsurface (upper few cm) geologic materials [1,2]. Examples of such physical properties include grain size (for unconsolidated sediment), degree of induration or cementation, vesicularity, porosity, or degree of fracturing. Many laboratory studies have related the physical properties of geologic particulates to their thermal properties [3-8]. However, methods have been inconsistent between laboratories and only a few studies have measured thermal properties in Mars-relevant pressures [e.g. 4]. Presley and Christensen conducted a number of studies [5-8] using a line-heat source apparatus in a Mars-like atmosphere and determined a quantitative relationship between unimodal and bimodal grain size samples and thermal properties. However, no thermal measurements at Mars pressures exist for solid samples, and quantitative relationships between thermal conductivity and rock porosity, mechanical strength [9], and density have not been determined for Mars conditions. This work aims to close the gaps in our understanding of thermal properties as they relate to physical characteristics of rocks and sediment on both Earth and Mars, while quantifying relationships between thermal properties on Earth and in Mars conditions for easier comparison of analog samples in the future.

**Samples:** We have gathered samples that span the chemical and physical range of rocks observed on Mars from a variety of sources, including volcanic vs. volcanoclastic, well-cemented vs. loosely consolidated sedimentary, and effusive vs. pyroclastic (**Table 1**). Additionally, we have obtained the same particulate samples used in the Presley and Christensen study that linked grain size and thermal conductivity for verification of our results. Samples

have been provided by D. Rogers, B. Thomson, R. Kronyak, G. Peters, E. Carey, D. McDougall, and S. Jaret. B. Thomson, R. Kronyak, G. Peters, and E. Carey provided rock mechanical strength measurements with their samples.

**Methods:** To measure thermal conductivity, we have obtained a C-Therm thermal conductivity TCi analyzer [10] and have built a bell-jar style vacuum chamber around it (see **Fig. 1** for setup). The sensor works as a modified transient plane heat source system; it uses interfacial heat reflectance by supplying heat to the sample and measuring the amount of heat reflected back to the sensor. C-Therm analyzers have been widely used in a number of industries (e.g., petroleum, pharmaceuticals, photovoltaics, textiles [10]) but this study represents the first time that they have been used in planetary thermal studies. At the time of writing, measurements have only been acquired under ambient pressure and temperatures (20-22 °C) due to early complications with the vacuum setup. We hope to present measurements conducted at Mars pressures by the time of the meeting.

Each sample must be cut and smoothed to have at least one flat surface that can sit flush on the sensor. The thermal measurements themselves do not alter a sample in any way, given that the temperature of the sensor changes by 1-2 °C. For measurements, contact agents are needed between the sensor and sample for any solid samples. These contact agents are normally distilled water for non-porous samples or Wakefield Thermal Joint Compound (a silicone oil-based grease) for porous samples. Individual thermal measurements take anywhere from 60-80 s and each sample has been measured in at least 3 different sessions for a total of 200 measurements for particulate samples and 300 for solid samples to reduce error due to contact agents.

Porosity measurements of selected samples were conducted at the Vatican Observatory. A Quantachrome Ultrapycnometer 1000 ideal-gas pycnometer was used with gaseous nitrogen, in which initial pressures in one chamber were compared with final pressures in the other sample-holding container to determine grain densities ( $\rho_g$ ). Bulk densities ( $\rho_b$ ) were measured using the NextEngine model 2020i Scanner HD Pro laser scanner and Geomagic Verify

software. Porosity ( $P$ ) was then calculated according to Eq 2.

$$P = 1 - (\rho_b/\rho_g) \quad (2)$$

A comparison of porosity and thermal properties is given in Fig. 3.

**Results:** Thermal inertia and conductivity results obtained at ambient pressures are summarized in Table 1 and in Figs. 2 and 3. Measurements are ongoing to determine the relationships of grain size, porosity, and mechanical strength with thermal properties at Mars pressures. Measurements of the highest thermal conductivities are still ongoing, which are largely the samples with rock mechanical strength data.

The discrepancy between our data and that predicted for these grain sizes by Presley and Christensen [5] may mean that the relationship they derived at low to moderate pressures (up to 100 mbar) does not hold for Earth-like pressures. Additionally, we observed a drop in density (not shown) that corresponded with the drop observed in thermal inertia/conductivity in larger grain sizes. We speculate that this is due to a porosity effect—larger grains stack in such a way that grain-to-grain contact surface area is reduced and pore space between grains increases. Therefore, the effect of the more sluggish conductivity through air overtakes the solid conductivity through grains.

#### References:

- [1] Wechsler, A. E. et al. (1972) *Characteristics of the Moon*, M. I. T. Press, 215-241. [2] Jakosky, B. M. (1986) *Icarus* 66, 117–124. [3] Wechsler, A. E., and Glaser, P. E. (1965) *Icarus* 4, 335–352. [4] Presley, M. A. and Christensen, P. R. (1997a) *JGR* 102, 6551–6566. [5] Presley, M. A. and Christensen, P. R. (1997b) *JGR* 107, 10-1–10-22. [6] Presley, M. A. and Craddock, R. A. (2006) *JGR* 111. [7] Presley, M. A. and Christensen, P. R. (2010a) *JGR* 115. [8] Presley, M. A. and Christensen, P. R. (2010b) *JGR* 115. [9] Thomson, B. J. et al. (2013) *JGR* 118, 1233–1244. [10] (2018) C-Therm thermal conductivity analyzer (TCi), C-Therm Technologies, Fredericton, NB, Canada.



**Fig. 1.** Laboratory setup at Stony Brook University in the Center for Planetary Exploration Spectroscopy Lab (left). The C-Therm TCi analyzer (right) sits within the bell-jar setup, and butterfly valves hold pressures to within 0.01 mb.

**Table 1.** Summary of samples used in this study. Those with dashes have measurements/information pending.

Sample	Porosity	k (W/mK)	I ( $J/m^2Ks^{1/2}$ )	Description	Locality
AND	8.8 ± 0.5	-	-	Andesite	
ANH-NS	-	-	-	Rock anhydrite	Nova Scotia, CAN
AR-SA	-	-	-	Argillaceous sandstone	Portageville, NY
BAS-01	15.1 ± 0.9	-	-	Aphanitic basalt	Prescott, AZ
BAS-02-1	13.0 ± 0.9	1.31	1580.91	Vesicular basalt	Keeler, CA
BAS-03	14.2 ± 0.5	-	-	Basalt	Mojave, CA
Bishop Tuff 049	38.5 ± 0.4	0.45	804.35	Tuff	Yosemite, CA
BTID 1	35.3 ± 0.6	0.05	131.02	Basaltic tuff	ID
BTID 7	22.1 ± 0.6	-	-	Basaltic tuff	ID
BTID 8	56.7 ± 0.5	0.05	131.77	Basaltic tuff	ID
C-ANT	14.7 ± 0.3	1.28	1555.00	Basaltic sandstone	Nunatak, Antarctica
Cerro Blanco 1	50.6 ± 0.5	0.06	150.77	Ignimbrite	near El Peñon, Argentina
Cerro Blanco 3	46.9 ± 0.2	0.36	711.14	Ignimbrite	near El Peñon, Argentina
Chapman Ridge Formation	2.0 ± 0.5	-	-	Sandstone	TN
China Ranch Gypsum	2.2 ± 0.4	-	-	Gypsum	Pahrump, NV
Clinch Formation	6.2 ± 0.3	-	-	Sandstone	TN
Cutler Formation	9.2 ± 0.6	2.68	2495.46	Fine-grained sandstone	UT
Gardnos breccia	32.7 ± 0.3	0.88	1213.11	Impact breccia	Gardnos impact, Norway
GRA	-	-	-	Graywacke	Grafton, NY
Juniata Formation	3.9 ± 0.4	-	-	Sandstone	TN
KAL-001-5	40.4 ± 0.4	1.05	1364.18	Kaolinite	Mammoth Mtn, CA
KMM-024-1	18.5 ± 0.3	0.12	283.50	Mudstone	Boron, CA
Lower Ridge Basin	4.2 ± 0.4	-	-	Fine-grained sandstone	Ridge Basin, CA
LS-01	25.9 ± 0.4	-	-	Limestone	Santa Barbara, CA
Middle Ridge Basin	18.4 ± 0.4	-	-	Sandstone	Ridge Basin, CA
Missoula Member	47.3 ± 0.3	0.43	782.38	Mudstone	MT
Morrison Formation	4.5 ± 0.3	-	-	Sandstone	UT
Napa Basaltic Sandstone	5.2 ± 0.2	-	-	Basaltic sandstone	Napa, CA
ODP-031-1	-	0.18	337.26	Pumice	Ridgecrest, CA
OOL	-	-	-	Siliceous oolite	State College, PA
Pumice	76.3 ± 0.6	0.08	200.56	Pumice	
Puna 4	68.9 ± 0.3	0.05	127.90	Pumice	near El Peñon, Argentina
Puna 5	58.1 ± 0.4	0.13	294.64	Pumice	near El Peñon, Argentina
SIL-CA	8.4 ± 0.6	-	-	Siltstone	Newhall, CA
SS-01	17.0 ± 0.5	2.16	2183.73	Sandstone	St. George, UT
Uniform Saddleback Basalt	-	-	-	Basalt	Boron, CA
Upper Ridge Basin	32.8 ± 0.4	0.09	230.94	Sandstone	Ridge Basin, CA
VB-ADR	54.1 ± 0.5	0.05	132.48	Vesicular basalt	
Wingate Formation	27.1 ± 0.1	1.29	1566.96	Sandstone	UT

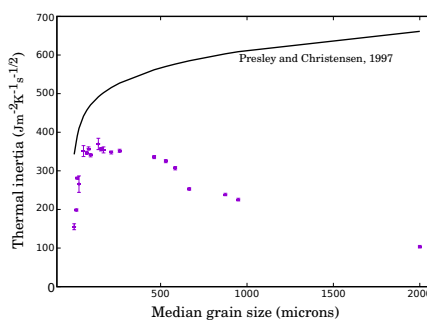


**Fig. 2.** Ambient pressure thermal inertia vs. grain size as measured in the C-Therm setup at SBU. The black line represents the Presley and Christensen [5] grain-size conductivity relationship calculated for a pressure of 1 bar. If data points appear to have no error bars, it is because the error is smaller than the data point itself.

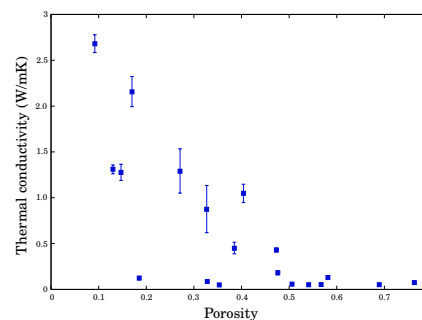


**Fig. 3.** Ambient-pressure thermal conductivity vs. porosity as measured in the C-Therm setup at SBU. If data points appear to have no error bars, it is because the error is smaller than the data point itself.